Available online at www.sciencedirect.com
SCIENCE DIRECT®
ELSEVIER
Thin Solid Films 460 (2004) 222–226
thin solid films
www.elsevier.com/locate/tsf

Microstructure of amorphous tantalum nitride thin films

S. Tsukimoto*, M. Moriyama, Masanori Murakami

Department of Materials Science and Engineering, Kyoto University Yoshida-honmachi, Sakyo-ku, Kyoto 606-8501, Japan

Received 7 July 2003; received in revised form 18 November 2003; accepted 15 January 2004
Available Online 25 March 2004

Abstract

The main purpose of the present microstructural analysis by transmission electron microscopy (TEM) and X-ray diffraction was to investigate whether amorphous TaN films are a potential candidate as diffusion barrier for Cu wiring used in Si devices. The TaN thin films were prepared by a sputter-deposition technique using Ar and N_2 mixed gas, and the film structure was found to be sensitive to the gas flow ratio of N_2 vs. Ar during sputtering. Polycrystalline TaN films were obtained when the $N_2/(Ar+N_2)$ ratio was smaller than 0.10 and amorphous TaN films were obtained when the ratio was larger than 0.15. Cross-sectional TEM observations revealed that the amorphous films had columnar structure with fine grains and that nano-scaled voids segregated at the boundaries. In addition, two-layered structures were observed in the amorphous TaN films and high density of the grain boundaries was formed close to the substrate. The present results suggested that the amorphous TaN films would not have high resistance against interdiffusion between two different materials because the density of grain boundaries with small voids was extremely high.
© 2004 Elsevier B.V. All rights reserved.

Keywords: Amorphous materials; Grain boundary; Tantalum nitride; Electron microscopy

1. Introduction

Tantalum nitride (TaN) thin films have been extensively used as the key elements of mask absorbers of X-ray lithography [1,2] and magnetic multilayers of recording heads [3]. Recently, demand to use TaN thin films as diffusion barrier layers for Cu wiring of Si semiconductor devices has increased because TaN films have excellent thermal stability [4–7]. With decreasing device dimensions, the thickness of the TaN diffusion barriers must decrease down to nanometers. For such extremely thin TaN films the dominant diffusion paths through the barriers were believed to be grain boundaries in the polycrystalline TaN films [5].

So far we have studied the barrier properties of polycrystalline TaN films [5] and did not pay attention to the barrier properties of amorphous TaN films because the amorphous TaN films were believed to have resistance against interdiffusion between two different materials higher than that of the polycrystalline films due to lack of the grain boundaries in the amorphous films.

The purpose of the present study was two-fold. The first was to propose a growth model for amorphous TaN films based on an understanding of the formation mechanisms. The second was to analyze the microstructure of the amorphous TaN films and to investigate the advantage and disadvantage of amorphous films as diffusion barriers in Si devices. The TaN thin films were prepared by the reactive sputter-deposition technique because TaN films were known to be extremely sensitive to the sputtering conditions [8,9]. TaN films with amorphous structure are expected to be prepared by adjusting the sputtering conditions. The films were characterized by X-ray diffraction (XRD) and transmission electron microscopy (TEM).

2. Experimental details

The substrates used in this study were (100)-oriented Si wafers. The wafers were chemically etched with diluted 5% HF solution and rinsed in deionized water and isopropyl alcohol prior to loading. Tantalum nitride thin films were prepared by reactive r.f. magnetron

*Corresponding author. Tel.: +81-75-753-5472; fax: +81-75-753-3579.
E-mail address: tsukimoto@micro.mtl.kyoto-u.ac.jp (S. Tsukimoto).

0040-6090/04/$ - see front matter © 2004 Elsevier B.V. All rights reserved.
doi:10.1016/j.tsf.2004.01.073

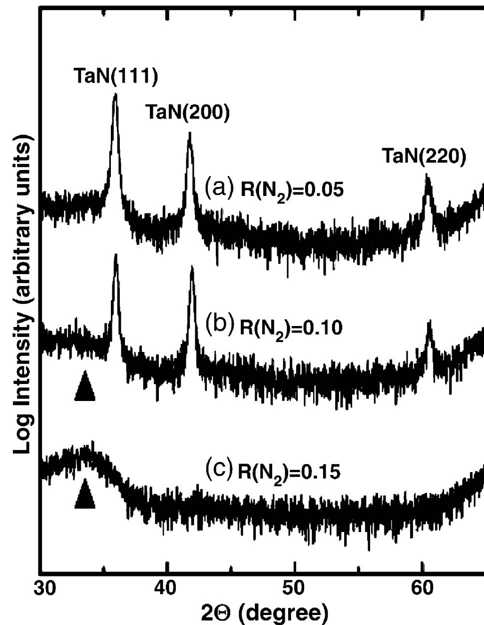

Fig. 1. XRD profiles of 30 nm-thick TaN films deposited on Si/SiO_x at various N_2 flow ratios to total flow, (a) $R(N_2)=0.05$, (b) 0.10 and (c) 0.15.

sputtering technique by sputtering a Ta target (99.99% purity) with Ar gas mixed with N_2 in predetermined ratios. The background pressure in the chamber was less than 5.3×10^{-6} Pa prior to deposition. The N_2 flow was varied between 0 and 5 sccm while the total gas ($Ar+N_2$) flow rate was kept at 20 sccm. During depositions, the sputtering power and the gas pressure were kept at 150 W and 2 Pa, respectively; the substrate holder was placed at 100 mm above the target. The thichnesses of the films were measured using cross-sectional TEM and the typical thickness was approximately 30 nm.

The XRD measurements with Cu Kα radiation were carried out to identify the structures of the deposited films. To characterize the microstructures at an atomic scale, both plan-view and cross-sectional high-resolution TEM observations were carried out using JEOL-4000EX at an accelerating voltage of 400 kV. For the plan-view TEM observations, the (100)-oriented Si wafers (with windows of 100 μm^2) coated with amorphous Si_3N_4 thin films (approx. 60 nm in thickness), were used as the substrate [10], which allowed observation without complicated specimen preparations. Thin foil specimens for the cross-section TEM observations were prepared by the standard procedures of cutting, gluing, mechanical grinding, dimple polishing, and Ar-ion sputter thinning at low angles of 6° and low energy of 3.0 kV in order to prevent radiation damages in the specimens.

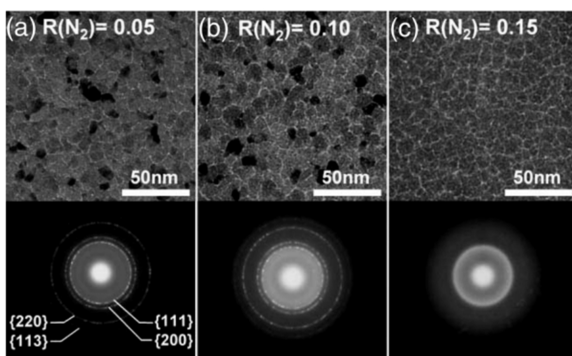

Fig. 2. (a) Plan-view bright field TEM images (upper) and diffraction patterns (lower) of the TaN films grown at $R(N_2)=0.05$, (b) 0.10, and (c) 0.15.

3. Experimental results and discussion

3.1. Deposition of amorphous tantalum nitride films

Fig. 1 shows the XRD profiles of the 30 nm-thick TaN films which were prepared by sputter-depositing on the Si/SiO_x substrates using various $N_2/(Ar+N_2)$ flow ratios (denoted as $R(N_2)$ hereafter). TaN film with a crystalline rock salt structure was formed when the film was prepared with a low $R(N_2)$ value of 0.05 as shown in Fig. 1a. Although peaks corresponding to the crystalline TaN were observed with increasing $R(N_2)$ value up to 0.10, the intensity ratio of $I(111)/I(200)$ decreased, which indicates that the (111) fiber structure became weaker with increasing the N_2 flow rate. Note that the diffuse scattering intensity at a diffraction angle of approximately $2\theta=34°$ slightly increases as indicated by an arrow in Fig. 1b for the films prepared with $R(N_2)=0.10$. At the $R(N_2)$ value of 0.15 (Fig. 1c), the diffuse scattering peak (shown by an arrow) increases while all Bragg diffraction peaks disappear within detection limit. These XRD profile changes with increasing the N_2 ratios are indicative of a film structural transition from crystalline to amorphous structure in the as-deposited TaN films. It is evident that the TaN film structure is very sensitive to the N_2 flow ratio. The present result of the sputtered TaN films is in good agreement with previous results reported by Lee et al. [11] and Stavrev et al. [12].

3.2. Columnar structure in amorphous TaN film

Fig. 2a–c show the plan-view bright field TEM images (upper) and the corresponding diffraction patterns (lower) of the TaN films prepared using the $R(N_2)$ values of 0.05, 0.10 and 0.15, respectively. The ring and diffused hallo diffraction patterns correspond to the polycrystalline and the amorphous TaN film structures, respectively. The crystalline film shown in Fig. 2a is composed of fine (crystalline) grains with ~10 nm in diameter. The coexistence of the crystalline and amorphous structures is observed in the film pre-

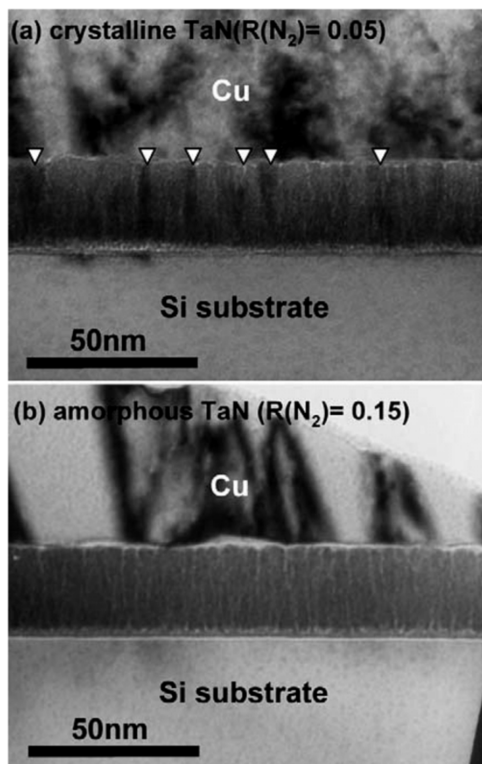

Fig. 3. Cross-sectional TEM images of the 30 nm-thick TaN films deposited on Si/SiO_x substrate, (a) crystalline TaN ($R(N_2)=0.05$), (b) amorphous TaN ($R(N_2)=0.15$).

pared using the N_2 ratio of 0.10 (Fig. 2b). Note that light 'network' contrast is observed along the grain boundaries as shown in Fig. 2a,b. The complete amorphous film structure is observed in Fig. 2c. This inhomogeneous microstructure with light network contrast in the amorphous film is similar to the grain boundaries in the crystalline film.

The cross-sectional TEM images of the 30 nm-thick crystalline and amorphous TaN films deposited on the Si/SiO_x substrate are shown in Fig. 3a,b, respectively. The copper layers were deposited on the TaN films to protect the TaN surface from damage during TEM specimen preparation. The thicknesses of the TaN films are quite uniform. The dark contrast regions in the Bragg-diffraction conditions shown by arrows in Fig. 3a and the light threading contrasts observed from the bottom to the top surface of the film indicate that the crystalline TaN film crystallizes in fine columnar grains. The amorphous TaN film has a threading contrast similar to that observed in the crystalline film, but the diffraction contrast from crystalline grains is not observed in Fig. 3b. From these TEM observations, the threading contrast observed in Fig. 3b could correspond to cross-sectional configuration of the grain boundaries in the columnar structure.

3.3. Formation of void network in columnar structure

Detailed analysis of the network contrast observed in the amorphous grain boundaries (Fig. 2c), was made by plan-view bright field TEM observation with in-focused, under-focused, and over-focused conditions. The amount of defocusing was ± 600 nm, where the negative and the positive signs represent the under- and over-focus conditions, respectively. The weak network contrast in the focused image is observed in Fig. 4a. The local non-uniform contrast is caused by the local fluctuation in the 'effective' film thickness such as film mass and thickness. This contrast is called mass-thickness contrast [13]. If the thickness of the amorphous film is uniform, the contrast is caused only by fluctuations in the local mass density. Therefore, this relatively broad network contrast represents density-deficient regions along the grain boundaries. In the under-focused image, light contrast dots forming a two-dimensional network are

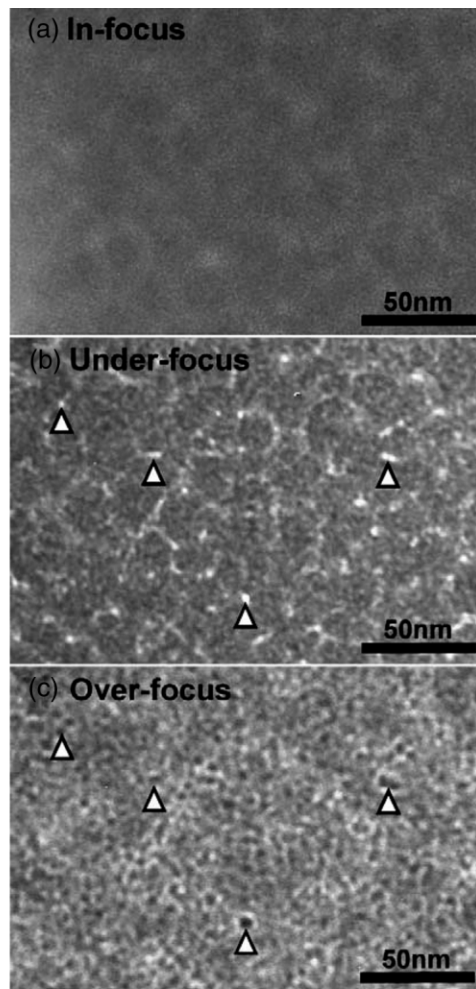

Fig. 4. Plan-view bright field TEM images of the amorphous TaN film taken in various defocus conditions Δf, (a) in-focus ($\Delta f=0$), (b) under-focus ($\Delta f=-600$ nm), and (c) over-focus ($\Delta f=+600$ nm).

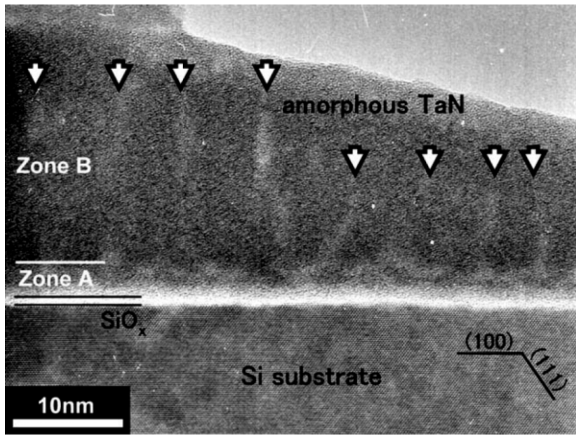

Fig. 5. Cross-sectional high-resolution TEM image of the amorphous TaN film deposited on Si/SiO_x substrate.

observed (Fig. 4b). However, these light dots convert to dark dots in the over-focus condition as indicated by arrows in Fig. 4c. The conversion in the contrast with defocusing is frequently observed at edges of porous TEM specimens and is known as Fresnel fringes. The fringes are generally produced in/near the regions where the inner potential/density changes abruptly [13]. The present TEM observation indicates that the dots observed in the amorphous TaN film are likely to correspond to region with density lower than that of the surrounding matrix (amorphous grains). Judging from the shapes of the contrast, the dots in the film are probably caused by nano-scale voids.

This void network structure was first observed by Donovan and Heineman in evaporated amorphous Ge thin films [14]. They have also observed the void structures in amorphous films of C, Ge, Si and various other compounds [15–19]. Donovan and Heineman suggested that the formation of the void network resulted in the density-deficient boundaries intrinsic in the amorphous film. Thus, the nano-scale voids in the amorphous TaN film could cause the void network structure observed in Fig. 4.

3.4. Layer structure of amorphous TaN film

To investigate the vertical structure of the amorphous TaN film a cross-sectional high-resolution TEM (HRTEM) observation was made for the amorphous TaN film prepared with $R(N_2)=0.15$ on the Si substrate which was covered by a native amorphous oxide (SiO_x) layer. No lattice fringe is visible in the HRTEM image of Fig. 5, confirming that the film has complete amorphous structure. The light threading contrasts caused by the grain boundaries are observed as indicated by arrows. Note that the columnar grain boundaries in the film do not pass through the film and are terminated at near the substrate. Highly dense light contrasts are observed close to the substrate surface within a thickness of $\sim$4 nm. From the cross-sectional TEM image, the microstructures in the amorphous TaN film are separated into two regions, which are denoted as zone-A and zone-B, respectively. Judging from the contrast distributions, the density of the grain boundaries in the zone-A is higher than that in the zone-B. Therefore, the zone-A region may be composed of very fine amorphous grains. Although this two-layered structure consisted of the columnar layer on the fine grain layer was previously observed in the polycrystalline TaN [20] and TiN films [21], it may be the first observation in the amorphous TaN films.

3.5. Growth mechanism of amorphous TaN films

Based on the present TEM observations, a film growth mechanism for the amorphous TaN film is schematically illustrated in Fig. 6. In the initial stages of film formation, low-mobility adatoms are agglomerated and the amorphous clusters are nucleated on the substrate (Fig. 6a). Subsequently, the clusters grow in the three-dimensional mode (island growth), the amorphous grains coalesce, and the zone-A region is formed (as shown in Fig. 6b). Small voids with high density may be formed at the grain boundaries of the zone-A near the substrate. These boundaries are density-deficient boundaries. This void formation mechanism was previously proposed by

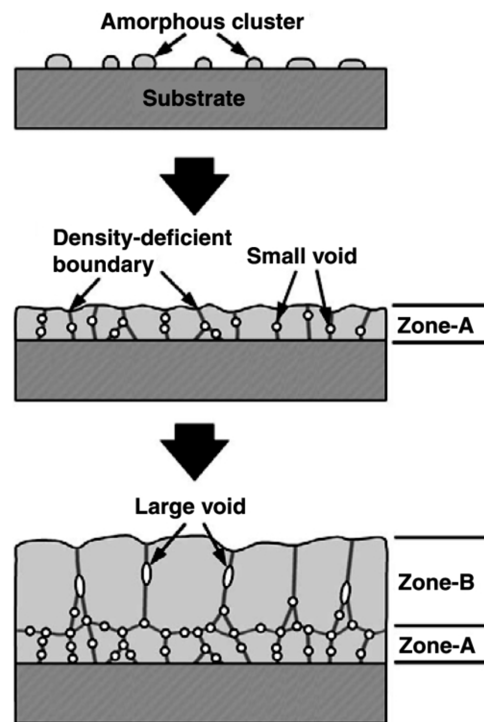

Fig. 6. Schematic illustrations indicated a sequence of the film growth and the void formation in the amorphous TaN film, (a) nucleation, (b) growth and coalescence, and (c) columnar growth.

Lloyd et al. [17] and Nakahara [18] as the coalescence-induced void formation mechanism (CVF). The amorphous grains coalesce at the expense of small grains and grow in the direction perpendicular to the substrate, resulting in the columnar grain formation. Large voids at the grain boundaries, as illustrated in the zone-B of Fig. 6c, will be formed during this columnar growth. Voids in the columnar structure would be formed both by the CVF mechanism and also by the shadowing effect during deposition [22]. As a consequence, the columnar grain structure with nano-scaled voids and density-deficient grain boundaries is most likely to be intrinsic in the deposited films.

This growth mechanism is similar to the model proposed by Movchan and Demchishin [23], and Thornton [22,24]. The Zone model developed by Thornton has been commonly applied to explain microstructures in sputtered films [24]. Both crystalline and amorphous TaN films were found to be composed of fine columnar grains by the present TEM observation. The microstructures of these TaN films may be classified as Zone-1 structure which is formed commonly in the films prepared at the substrate temperature of $T_s/T_m<0.3$, because the present films were prepared at the substrate temperature T_s of approximately 300 K (T_m is the melting point (=3360 K) of TaN). This Zone model can be applied to the microstructures in the present amorphous TaN film growth. The amorphous cadmium arsenide (Cd_3As_2) film was one of the typical examples which were reported to grow by the Zone model [25].

4. Conclusions

Microstructural analysis was carried out on amorphous TaN thin films prepared by sputtering Ta targets using Ar and N_2 mixed gas. It was found that the structures of the TaN films were sensitive to the N_2 gas flow ratio during sputtering and complete amorphous films were prepared with high N_2 flow ratio of $R(N_2)=0.15$. Based on high-resolution cross-sectional TEM observation, the growth model of the amorphous films was found to be similar to the Thornton's Zone model. However, it was found that the amorphous film had columnar structure with grain boundaries similar to those of the polycrystalline film. In addition, two distinct layers were observed: the bottom layers (close to the substrate) had high density grain boundaries and the top columnar layers had relatively low density grain boundaries. Micro-voids were observed to segregate at the grain boundaries.

From the present study, it was suggested that the amorphous TaN films do not necessarily show excellent diffusion barrier properties compared with the polycrystalline films, because grain boundaries with low mass density observed in the amorphous films might be dominant diffusion paths.

Acknowledgments

This work was partially supported by Nanotechnology program on Cu Thin Films from the New Energy and Industrial Technology Development Organization (NEDO) of Japan.

References

[1] T. Yoshihara, S. Kotsuji, K. Suzuki, J. Vac. Sci. Technol. B 14 (1996) 4363.
[2] S.Y. Lee, C.M. Park, J. Ahn, Jpn. J. Appl. Phys. 39 (2000) 6919.
[3] S. Li, P.P. Freitas, M.S. Rogalski, M. Azevedo, J.B. Sousa, Z.N. Dai, J.C. Soares, N. Matsakawa, H. Sakakima, J. Appl. Phys. 81 (1997) 4501.
[4] J.O. Olowolafe, C.J. Mogab, R.B. Gregory, M. Kottke, J. Appl. Phys. 72 (1992) 4099.
[5] T. Oku, E. Kawakami, M. Uekubo, K. Takahiro, S. Yamaguchi, M. Murakami, Appl. Surf. Sci. 99 (1996) 265.
[6] M.H. Tsai, S.C. Sun, C.E. Tsai, S.H. Shuang, H.T. Chiu, J. Appl. Phys. 79 (1996) 6932.
[7] M. Stavrev, D. Fischer, F. Praessler, C. Wenzel, K. Drescher, J. Vac. Sci. Technol. A 17 (1999) 993.
[8] O.Yu. Khyzhun, Ya.V. Zaulychny, Phys. Status Solidi B 207 (1998) 191.
[9] X. Sun, E. Kolawa, J.S. Chen, J.S. Reid, M.A. Nicolet, Thin Solid Films 236 (1993) 347.
[10] T.S. Kuan, M. Murakami, Metall. Trans. A 13A (1982) 383.
[11] W.H. Lee, J.C. Lin, C. Lee, Mater. Chem. Phys. 68 (2001) 266.
[12] M. Stavrev, D. Fischer, C. Wenzel, K. Drescher, N. Mattern, Thin Solid Films 307 (1997) 79.
[13] D.B. Williams, C.B. Carter, Transmission Electron Microscopy: A Textbook for Materials Science, Plenum Press, New York, 1996.
[14] T.S. Donovan, K. Heinemann, Phys. Rev. Lett. 27 (1971) 1794.
[15] J.J. Hauser, A. Staudinger, Phys. Rev. B 7 (1973) 607.
[16] A. Staudinger, S. Nakahara, Thin Solid Films 45 (1977) 125.
[17] J.R. Lloyd, S. Nakahara, J. Vac. Sci. Technol. 14 (1977) 655.
[18] S. Nakahara, Thin Solid Films 45 (1977) 421.
[19] R. Messier, R.C. Ross, J. Appl. Phys. 53 (1982) 6220.
[20] C.S. Shin, D. Gall, Y.W. Kim, N. Hellgren, I. Petrov, J.E. Greene, J. Appl. Phys. 92 (2002) 5084.
[21] M. Moriyama, T. Kawazoe, M. Tanaka, M. Murakami, Thin Solid Films 416 (2002) 136.
[22] J.A. Thornton, J. Vac. Sci. Technol. A 4 (1986) 3059.
[23] B.A. Movchan, A.V. Demchishin, Phys. Met. Metallogr. 28 (1969) 83.
[24] J.A. Thornton, J. Vac. Sci. Technol. 11 (1974) 666.
[25] J. Jurusik, L. Zdanowicz, Thin Solid Films 144 (1986) 241.